

Supplementary Information

Pt(II)-activated coupling of aminoethylferrocene with benzonitrile. A facile access route to a new redox-active bis(ferrocenyl-amidine) anion sensor

Daniel Nieto,^a Ana M^a González-Vadillo,^{*a} Sonia Bruña,^a César J. Pastor,^b

Angel E. Kaifer^{*c} and Isabel Cuadrado^{*a}

^a Departamento de Química Inorgánica, Facultad de Ciencias, ^b Laboratorio de Difracción de Rayos X, Universidad Autónoma de Madrid, Cantoblanco, 29049, Madrid, Spain. E-mail: isabel.cuadrado@uam.es

^c Center for Supramolecular Science and Department of Chemistry, University of Miami, Coral Gables, FL 33124-0431, USA. E-mail: akaifer@miami.edu

1. General Experimental Details	2
1.1. Materials and Equipment	2
1.2. Electrochemical Measurements and Titrations	2
1.3. X-ray Crystal Structure Determination	3
2. Synthetic Procedures	4
2.1. Synthesis of <i>cis</i> -Bis(benzonitrile)dichloroplatinum(II)	4
2.2. Synthesis of β -aminoethylferrocene (1)	4
2.3. Synthesis of <i>trans</i> -[PtCl ₂ {NH=C(Ph)NH(CH ₂) ₂ Fe(η^5 -C ₅ H ₄)(η^5 -C ₅ H ₅)} ₂](2)	4
2.4. Synthesis of <i>trans</i> -[PtCl ₂ (NCPh){NH=C(Ph)NH(CH ₂) ₂ Fe(η^5 -C ₅ H ₄)(η^5 -C ₅ H ₅)} ₂](3)	5
3. Structural Characterization of Compounds 1, 2 and 3	6
Figures S1 and S2: ¹ H NMR and ¹³ C NMR spectra of 1	6
Figures S3 and S4: HMQC and HMBC NMR spectra and FAB spectrum of 1	7
Figures S5 and S6: ¹ H NMR and ¹³ C NMR spectra of 2	8
Figures S7 and S8: ¹⁹⁵ Pt NMR and IR spectra of compound 2	9
Figure S9: Mass spectrometry characterization by ESI for compound 2	10
Figures S10, S11 and: ¹ H NMR and ¹³ C NMR spectra of 3	11
Figures S12, S13 and S14: ¹⁹⁵ Pt NMR, IR and Mass spectrum of compound 3	12
4. Crystallographic Data for Compound 2	13
Table S1: Selected crystallographic data for 2	13
Figure S15: Crystal-packing diagram of 2	14
5. Electrochemistry of Compound 2	15
Figures S16 and S17: CVs of 2 in CH ₂ Cl ₂ and CH ₃ CN/CH ₂ Cl ₂ (2.5:0.5 v)	15
Figure S18: Effect of H ₂ PO ₄ ⁻ on the electrochemical responses of 2	16
Figure S19, S20 and S21: Effect of F ⁻ , CH ₃ COO ⁻ and HSO ₄ ⁻ on the electrochemical responses of 2	17
Figure S22: SWV response of 2 in the presence of: F ⁻ + CH ₃ COO ⁻ + HSO ₄ ⁻ + H ₂ PO ₄ ⁻	18
6. Electrochemistry of Compound 3	19
Figure S23: CVs of 3 in CH ₂ Cl ₂	19
Figure S24: Effect of H ₂ PO ₄ ⁻ on the electrochemical responses of 3	19
7. References	20

1. General Experimental Details

1.1 Materials and Equipment. All reactions and compound manipulations were performed in an oxygen- and moisture-free atmosphere (N_2 or Ar) using standard Schlenk techniques. Solvents were dried by standard procedures over the appropriate drying agents and distilled immediately prior to use. Platinum(II) chloride, benzonitrile (Aldrich), potassium cyanide, aluminium chloride (Fluka), N,N,N -(ferrocenylmethyl) trimethylammonium iodide and lithium aluminium hydride (Alfa Aesar) were used as received. Phosphorus trichloride and pyridine (Aldrich) were distilled prior to use. Silica gel 60 silanized (0.063–0.200 mm) (Merk) and silica gel (70–230 mesh) (Aldrich) were used for column chromatographic purifications. Tetrabutylammonium salts were obtained in their anhydrous forms (Aldrich, Fluka).

Infrared spectra were recorded on Bomem MB-100 FT-IR and on Perkin Elmer 100 FT-IR spectrometers. 1H , ^{13}C , ^{195}Pt NMR spectra, as well as bidimensional spectra, were recorded on a Bruker-AMX-300 and Bruker-DRX-500 spectrometers. Chemical shifts were reported in parts per million (δ) with reference to residual solvents resonances for 1H and ^{13}C NMR ($CDCl_3$: 1H , δ 7.27 ppm, ^{13}C , δ 77.0 ppm; and CD_2Cl_2 : 1H , δ 5.33 ppm, ^{13}C , δ 53.8 ppm). Electrospray ionization (ESI) mass spectra were recorded with a QSTAR (Applied Biosystems) spectrometer, using methanol as ionizing phase, while FAB-mass spectra were obtained by using a VG AutoSpec (Waters) mass spectrometer with m-NBA as the matrix. Samples were prepared in CH_2Cl_2 . Elemental analyses were performed by the Microanalytical Laboratory, SIDI, Universidad Autónoma de Madrid, Spain.

1.2 Electrochemical Measurements. Cyclic voltammetric and square wave voltammetric experiments were recorded on a BAS-CV-50W potentiostat. CH_2Cl_2 and CH_3CN (spectrograde) for electrochemical measurements were freshly distilled from calcium hydride under argon. The supporting electrolyte was tetra-*n*-butylammonium hexafluorophosphate (Fluka), which was purified by recrystallization from ethanol and dried in vacuum at 60 °C. The supporting electrolyte concentration was typically 0.1 M. A conventional three-electrode cell connected to an atmosphere of prepurified nitrogen was used. All cyclic voltammetric experiments were performed using either a platinum-disk working electrode ($A = 0.020\text{ cm}^2$) or a glassy carbon-disk working electrode ($A = 0.070\text{ cm}^2$) (both Bioanalytical Systems), each of which were polished on a Buehler polishing cloth with Metadi II diamond paste, rinsed thoroughly with purified water and acetone, and dried. A coiled platinum wire was used as a counter electrode. Solutions were 10^{-3} M in the redox active specie. The solutions for the electrochemical experiments were deoxygenated by bubbling nitrogen for at least 10 min and kept under an inert atmosphere throughout the measurements. All potentials were referenced to the saturated calomel electrode (SCE). Under our conditions, the decamethylferrocene redox couple $[FeCp^*_2]^{0/+}$ is 0.55 V vs SCE in $CH_2Cl_2/0.1\text{ M }[n\text{-Bu}_4N][PF_6]$. Square wave voltammetry (SWV) was performed using frequencies of 10 Hz.

Electrochemical Titrations. A solution (3 mL) of compound **2** or **3** (5×10^{-4} or 10^{-3} M) and 0.1 M of $[Bu_4N][PF_6]$ was placed in an electrochemical cell, purged with nitrogen for at least 10 min, and stirred. Stirring was stopped and a nitrogen atmosphere was maintained above the solution while the experiment was in progress. The electrodes were cleaned after each run. Anion recognition studies were performed by consecutive additions of variable molar equiv of each tetrabutylammonium salt of the anion guest. Tetrabutylammonium salts of the monovalent anions acetate, dihydrogenphosphate, hydrogensulphate and fluoride were employed for this work.

1.3 X-ray Crystal Structure Determination. Compound **2** was structurally characterized by single-crystal X-ray diffraction. A suitable orange crystal of **2** of dimensions $0.18 \times 0.14 \times 0.07$ mm, was located and mounted on a glass fiber with “magic oil”. The sample was transferred to a Bruker SMART 6K CCD area-detector three-circle diffractometer with a MacScience rotating anode (Cu K α radiation, $\lambda = 1.54178$ Å) generator equipped with Goebel mirrors at settings of 50 kV and 100 mA. A total of 3057 independent reflections ($R_{\text{int}} = 0.0314$) were collected in the range $3.75^\circ < \theta < 69.34^\circ$. X-ray data were collected at 100 K, with a combination of six runs at different φ and 2θ angles, 3600 frames. Data were collected using 0.3° wide ω scans with a crystal-to-detector distance of 4.0 cm. The substantial redundancy in data allows empirical absorption corrections (SADABS)¹ to be applied using multiple measurements of symmetry-equivalent reflections. Raw intensity data frames were integrated with the SAINT program,² which also applied corrections for Lorentz and polarization effects. The software package SHELXTL version 6.10 was used for space group determination, structure solution and refinement.³ The space group determination was based on a check of the Laue symmetry and systematic absences and was confirmed using the structure solution. The structure was solved by direct methods (SHELXS-97), completed with difference Fourier syntheses, and refined with full-matrix least-squares using SHELXL-97 minimizing $w(F_o^2 - F_c^2)$.^{4,5} Weighted R factors (R_w) and all goodness of fit S are based on F^2 ; conventional R factors (R) are based on F . All non-hydrogen atoms were refined with anisotropic displacement parameters. The hydrogen atom positions were calculated geometrically and were allowed to ride on their parent carbon atoms with fixed isotropic U . All scattering factors and anomalous dispersion factors are contained in the SHELXTL 6.10 program library. The crystal structure of **2** has been deposited at the Cambridge Crystallographic Data Centre and allocated the deposition number CCDC 822240.

2. Synthetic procedures

2.1. Synthesis of *cis*-bis(benzonitrile)dichloroplatinum(II). Isomerically pure *cis*-[PtCl₂(PhCN)₂] was prepared by reaction of anhydrous PtCl₂ and neat benzonitrile by adapting the literature procedure.⁶ A mixture of anhydrous platinum(II) chloride (0.5 g, 1.9 mmol) and C₆H₅CN (16 mL, excess) was stirred for 24 h at 30 °C. The reaction mixture was cooled to –30 °C. A yellow solid precipitated overnight which was collected by filtration and washed with small portions of *n*-hexane. The solid was dissolved in CH₂Cl₂ and filtered to remove any solid impurities. After solvent removal, a yellow solid product was obtained which was purified by chromatography on a 3 cm × 30 cm silica gel column (70–230 mesh). A minor first band containing *trans*-[PtCl₂(PhCN)₂] was eluted using CH₂Cl₂. Subsequently, a second major band was eluted using the same solvent. Solvent removal afforded the desired compound *cis*-[PtCl₂(PhCN)₂] as a needle-like yellow crystalline solid. Yield: 480 mg (54%). ¹H NMR (CD₂Cl₂, 300MHz): δ 7.82 (4H, m, *o*-Ph), 7.76 (2H, m, *p*-Ph), 7.59(4H, m, *m*-Ph). IR (KBr): ν(C≡N) 2285cm⁻¹, ν(Pt–Cl) 358, 348 cm⁻¹.

2.2. Synthesis of β-aminoethylferrocene, Fe{[(η⁵-C₅H₄)(CH₂)₂NH₂](η⁵-C₅H₅)} (1)

Monofunctionalized 2-aminoethylferrocene (**1**) was synthesized in two steps from commercially available N,N,N-trimethylferrocenylmethylammonium iodide, by adapting the literature procedures.^{7,8}

1-cyanomethylferrocene⁷ (5.55 g, 24.4 mmol) in dry diethyl ether (90 ml) was added dropwise to a stirred suspension of LiAlH₄ (1.63 g, 43 mmol) in 100 mL of dry diethyl ether and heated at 35 °C. After being stirred for 3 h under reflux, the reaction mixture was externally cooled with an ice bath, and cold water was slowly added dropwise until H₂ release stopped. Once decanted, the solution was acidified by addition of H₂SO₄ 6M. The solid formed was separated by filtration and treated with an 6N NaOH aqueous solution to adjust the pH ≈ 11. The dark orange mixture was extracted with diethyl ether, the organic phases were combined, dried (over Na₂CO₃) and filtered and the solvent was removed under vacuum. A viscous brown oil was obtained which was dissolved in *n*-hexane and filtered to remove any solid impurities. Solvent removal afforded compound **1** as a viscous oily dark red product, which can be purified by distillation in vacuum. Yield: 3.7 g (66%). ¹H NMR (CDCl₃, 300MHz): δ 1.30 (s br, 2H, NH₂), 2.50 (t, ³J = 7.0 Hz, 2H, Fe–CH₂), 2.80 (t, ³J = 7.0 Hz, 2H, CH₂–NH₂), 4.07, 4.08 (m, 4H, C₅H₄), 4.10 (s, 5H, C₅H₅). ¹³C{¹H} NMR (CDCl₃, 75MHz): δ 34.1 (Fe–CH₂), 43.6 (CH₂–NH₂), 67.4, 68.4, 86.3 (C₅H₄), 68.6 (C₅H₅). IR (CsI): ν(N–H) 3368, 3292 cm⁻¹, ν(C–H) 3091, 2927, 2853 cm⁻¹, δ(N–H) 1587 cm⁻¹, δ(C–H) 818 cm⁻¹, ρ(Fe–Ring) 483 cm⁻¹.

2.3. Synthesis of *trans*-[PtCl₂{NH=C(Ph)NH(CH₂)₂Fe(η⁵-C₅H₄)(η⁵-C₅H₅)}₂] (2). A solution of **1** (194.5 mg, 0.849 mmol) in 4 mL of dry CH₂Cl₂ was added, via cannula, to a stirred solution of *cis*-[PtCl₂(PhCN)₂] (160 mg, 0.339 mmol) in 10 mL of CH₂Cl₂. The reaction mixture was stirred for 24 h at room temperature and then at 35 °C for additional 7 h. The solution was cooled to –30 °C for 24 h giving a brown solid which was filtered off, washed with *n*-hexane and purified by a silanized silica gel column chromatography (2 cm × 13 cm). A mayor yellow-orange band was eluted with *n*-hexane/CH₂Cl₂ (2:1). Solvent removal afforded compound **2** as an analytically pure air-stable orange needle-like crystalline solid. Yield: 190 mg (60%). Anal. Calc. For C₃₈H₄₀Cl₂Fe₂N₄Pt: C, 49.05;

H, 4.33; N, 6.02 %. Found: C, 49.32; H, 4.49; N, 5.72 %. ^1H NMR (300 MHz, CD_2Cl_2): δ 7.87 (2H, br, PtNH), 7.53 (2H, m, *p*-Ph), 7.47 (4H, m, *o*-Ph), 7.33 (4H, m, *m*-Ph), 5.59 (2H, br, $\text{NHCH}_2\text{CH}_2\text{Fc}$), 4.13, 4.11 (8H, m, C_5H_4), 4.07 (10H, s, C_5H_5), 3.25 (4H, m, CH_2NH), 2.59 (4H, m, FcCH_2). $^{13}\text{C}\{^1\text{H}\}$ NMR (75 MHz, CD_2Cl_2): δ 170.5 (*ipso*- NHCNH), 133.9 (*ipso*-Ph), 131.1 (*p*-Ph), 129.2 (*o*-Ph), 127.6 (*m*-Ph), 85.1 (*ipso*-Fc), 69.0, 68.0 (C_5H_4), 68.9 (C_5H_5), 46.4 (CH_2NH), 31.1 (FcCH_2). ^{195}Pt NMR (64 MHz, CD_2Cl_2): δ -2020. IR (KBr): $\nu(\text{N-H})$ 3347–3209 cm^{-1} , $\nu(\text{C-H})$ 3088–2924 cm^{-1} , $\nu(\text{C=N})$ 1618 cm^{-1} , $\delta(\text{N-H})$ 1575 cm^{-1} , $\delta(\text{C-H})$ 707 cm^{-1} , $\rho(\text{Fe-Ring})$ 483 cm^{-1} , $\nu(\text{Pt-Cl})$ 325 cm^{-1} . MS (ESI^+): m/z 929.09 [M^+], 894.13 [$\text{M-Cl}]^+$, 857.15 [$\text{M-2Cl}]^+$, 333.11 [$\text{Fc}(\text{CH}_2)_2\text{NHC}(\text{C}_6\text{H}_5)\text{NH}]^+$.

2.4. Synthesis of *trans*-[PtCl₂(N≡CPh){NH=C(Ph)NH(CH₂)₂Fe(η^5 -C₅H₄)(η^5 -C₅H₅)}] (3). A solution of **1** (108.0 mg, 0.471 mmol) in 3 mL of dry CH_2Cl_2 was added, via cannula, to a stirred solution of *cis*-[PtCl₂(PhCN)₂] (222.0 mg, 0.471 mmol) in 10 mL of CH_2Cl_2 . The reaction mixture was stirred for 24 h at 35 °C. The solvent was evaporated under reduced pressure affording a dark orange solid, which was purified by column chromatography (2 cm × 13 cm) on silanized silica gel. A mayor yellow band was eluted with *n*-hexane/ CH_2Cl_2 (5:1). Solvent removal afforded compound **3** as an analytically pure air-stable yellow crystalline solid. Yield: 162 mg (49%). Anal. Calc. For $\text{C}_{26}\text{H}_{25}\text{Cl}_2\text{FeN}_3\text{Pt}$: C, 44.53; H, 3.59; N, 5.99 %. Found: C, 44.84; H, 3.71; N, 5.68 %. ^1H NMR (300 MHz, CD_2Cl_2): δ 8.08 (1H, br, PtNH), 7.78 (2H, m, *o*-PhC≡N), 7.72 (1H, m, *p*-PhC≡N), 7.56 (2H, m, *m*-PhC≡N), 7.50 (1H, m, *p*-PhC≡N), 7.45 (2H, m, *o*-PhC≡N), 7.26 (2H, m, *m*-PhC≡N), 5.51 (1H, br, $\text{NHCH}_2\text{CH}_2\text{Fc}$), 4.08 (4H, s, C_5H_4), 4.03 (5H, s, C_5H_5), 3.21 (2H, m, CH_2NH), 2.56 (2H, m, FcCH_2). $^{13}\text{C}\{^1\text{H}\}$ NMR (125 MHz, CD_2Cl_2): δ 170.5 (*ipso*- NHCNH), 134.7 (*p*-PhC≡N), 133.4 (*o*-PhC≡N), 132.7 (*ipso*-PhC≡N), 131.0 (*p*-PhC≡N), 129.4 (*m*-PhC≡N), 128.9 (*o*-PhC≡N), 127.3 (*m*-PhC≡N), 116.5 (C≡N), 110.0 (*ipso*-PhC≡N), 84.4 (*ipso*-Fc), 68.6, 67.7 (C_5H_4), 68.5 (C_5H_5), 46.3 (CH_2NH), 30.7 (FcCH_2). ^{195}Pt NMR (64 MHz, CD_2Cl_2): δ -2177. IR (KBr): $\nu(\text{N-H})$ 3349–3276 cm^{-1} , $\nu(\text{C-H})$ 3086–2924 cm^{-1} , $\nu(\text{C}\equiv\text{N})$ 2283 cm^{-1} , $\nu(\text{C=N})$ 1624 cm^{-1} , $\delta(\text{N-H})$ 1576 cm^{-1} , $\delta(\text{C-H})$ 705 cm^{-1} , $\rho(\text{Fe-Ring})$ 484 cm^{-1} , $\nu(\text{Pt-Cl})$ 327 cm^{-1} . MS (ESI^+): m/z 723.03 [$\text{M+Na}]^+$, 700.05 [M^+], 628.09 [$\text{M-2Cl-H}]^+$, 525.05 [$\text{M-2Cl-H-NCPh}]^+$.

3. Structural Characterization of Compounds 1, 2 and 3.

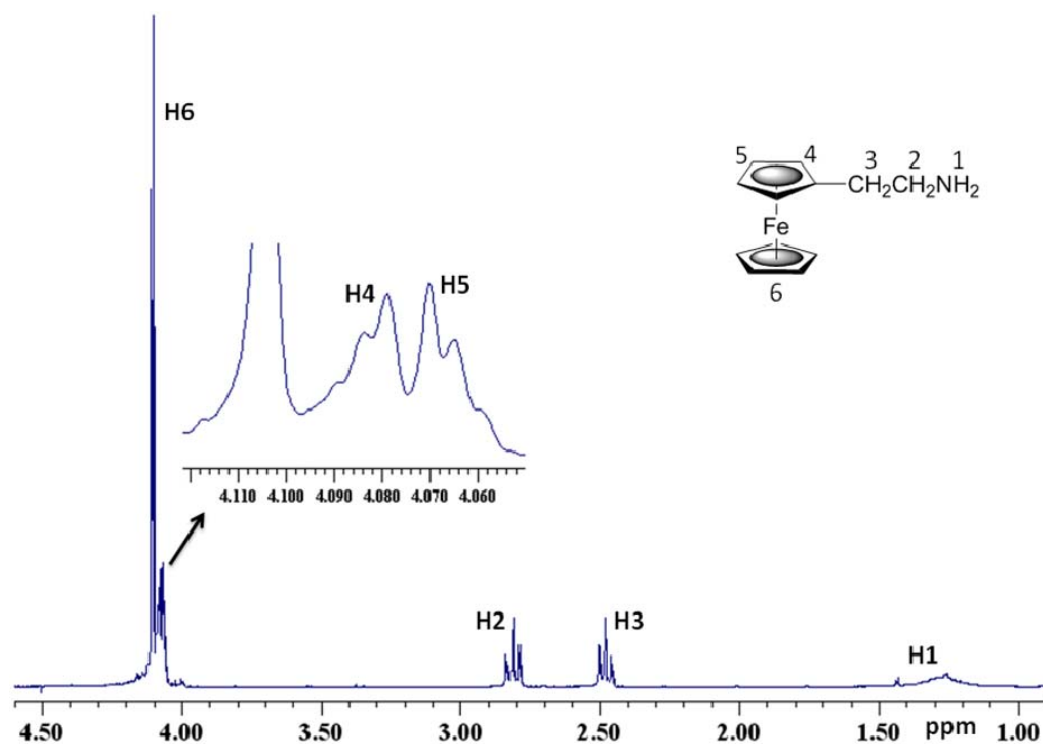


Figure S1. ^1H NMR spectrum (in CDCl_3 , 300 MHz) of compound **1** (inset: expanded view of cyclopentadienyl region).

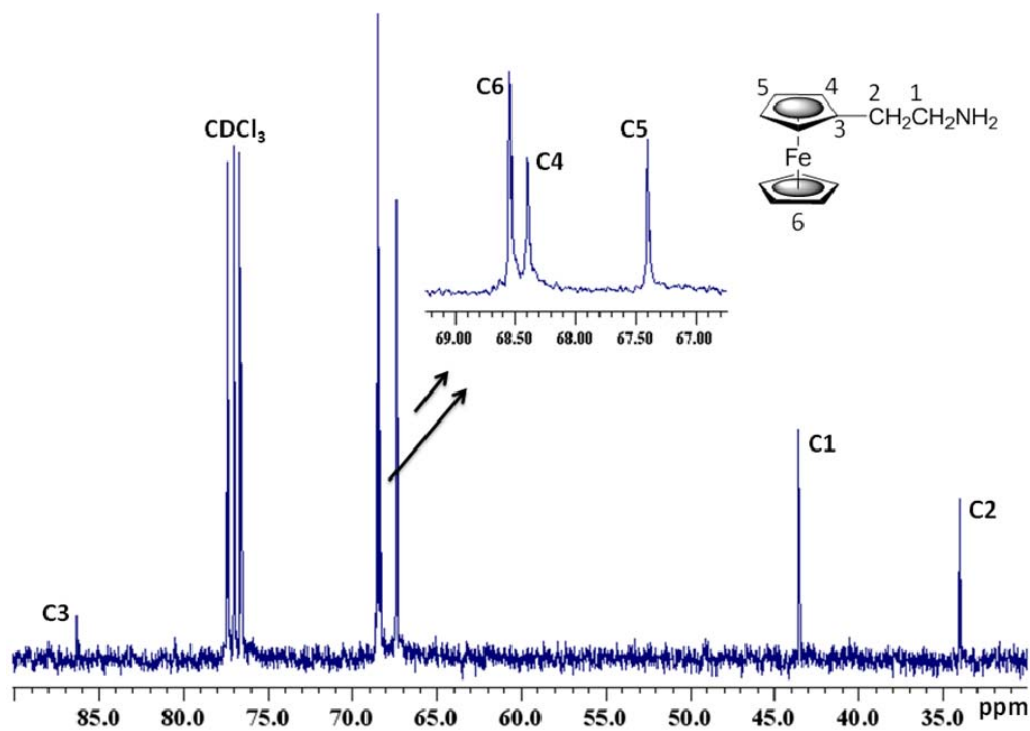


Figure S2. ^{13}C NMR spectrum (in CDCl_3 , 75 MHz) of compound **1** (inset: expanded view of cyclopentadienyl region).

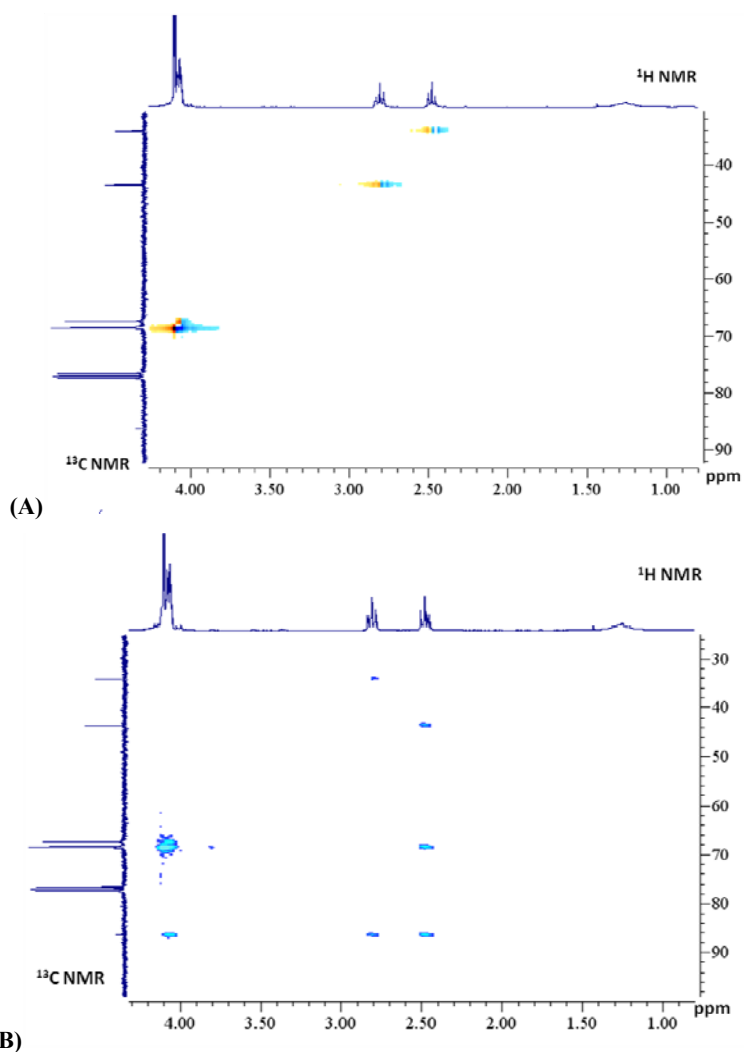


Figure S3. HMQC NMR spectrum (A) and HMBC NMR spectrum (B) (in CDCl_3 , 300 MHz) of **1**.

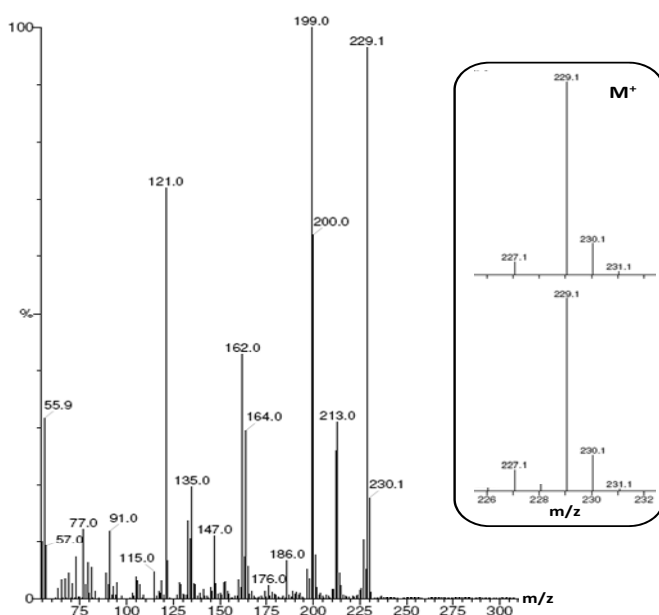
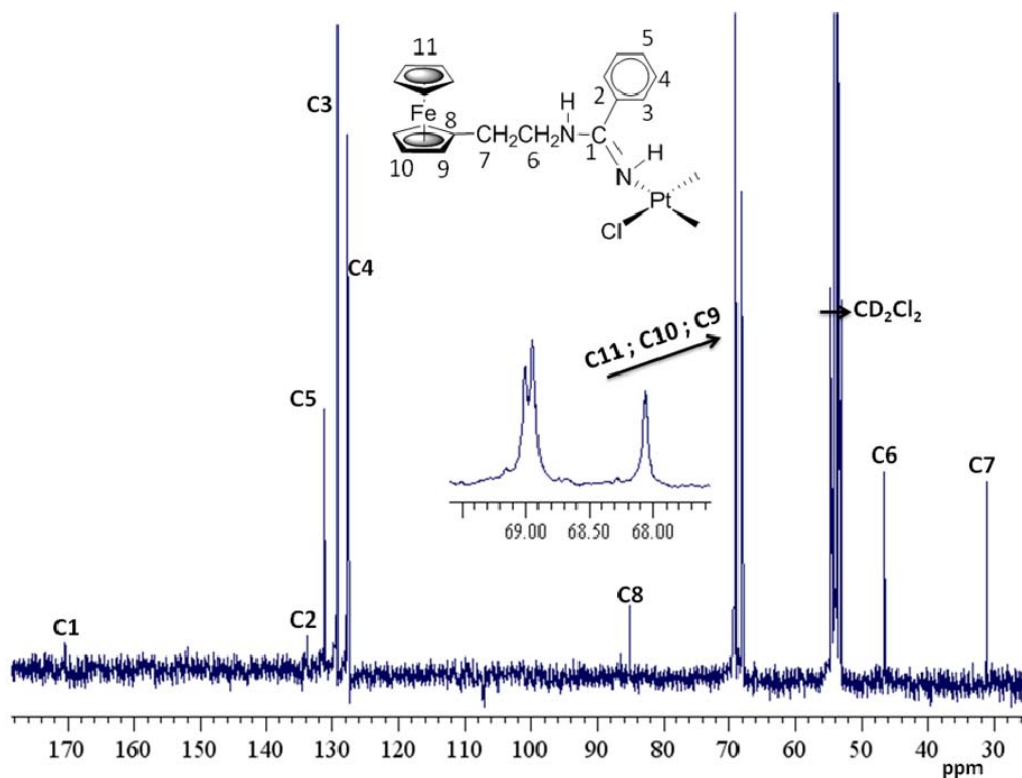
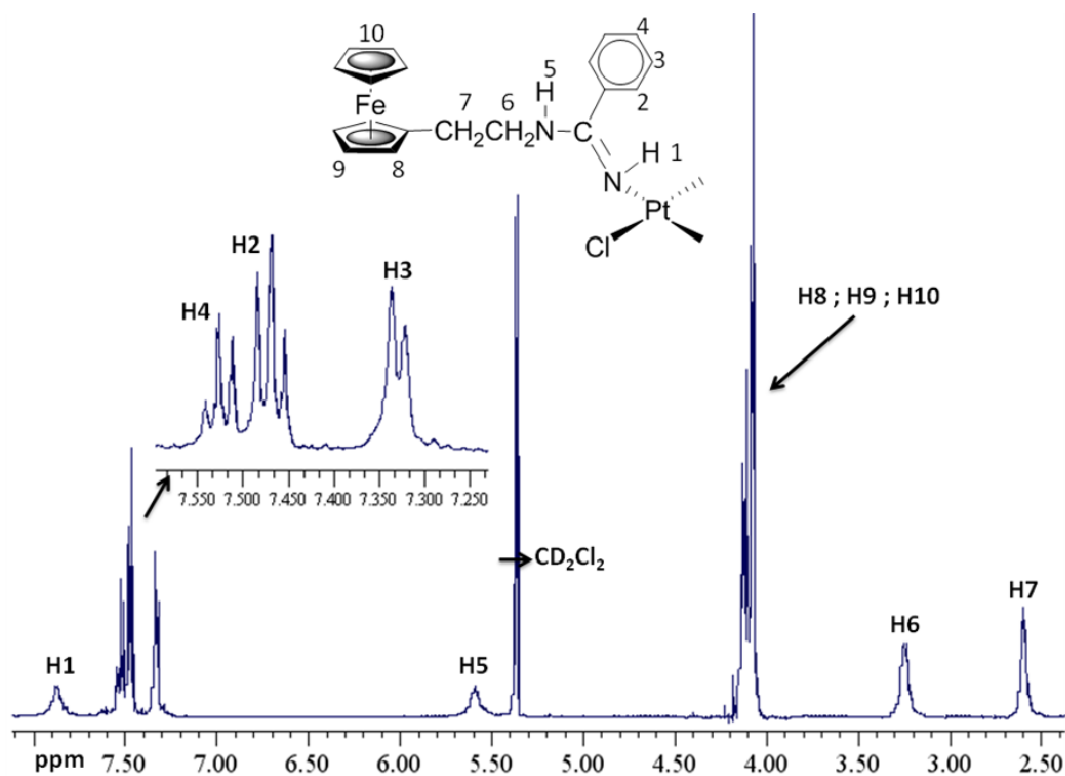


Figure S4. FAB spectrum of **1**. Inset: isotopic distribution of molecular peak, calculated (bottom) and experimental (top).



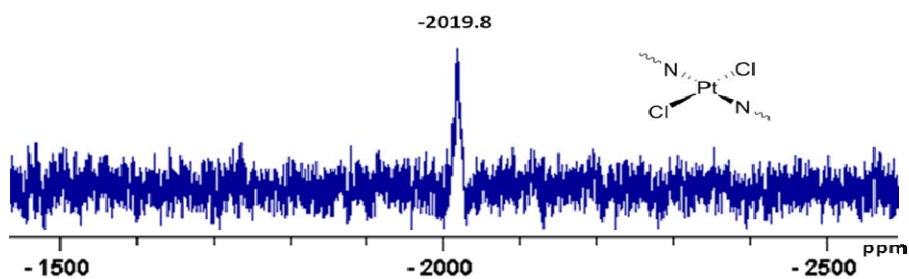


Figure S7. ^{195}Pt NMR spectrum (in CD_2Cl_2 , 64 MHz) of compound **2**.

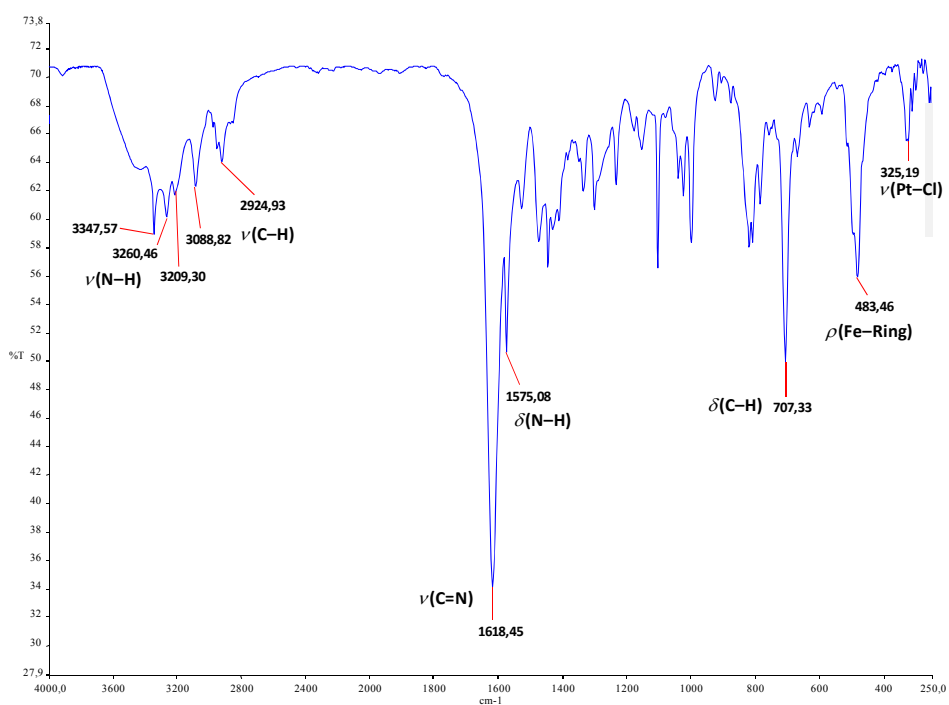


Figure S8. IR spectrum (in KBr) of compound **2**.

Electronic Supplementary Material (ESI) for Chemical Communications
This journal is (c) The Royal Society of Chemistry 2011

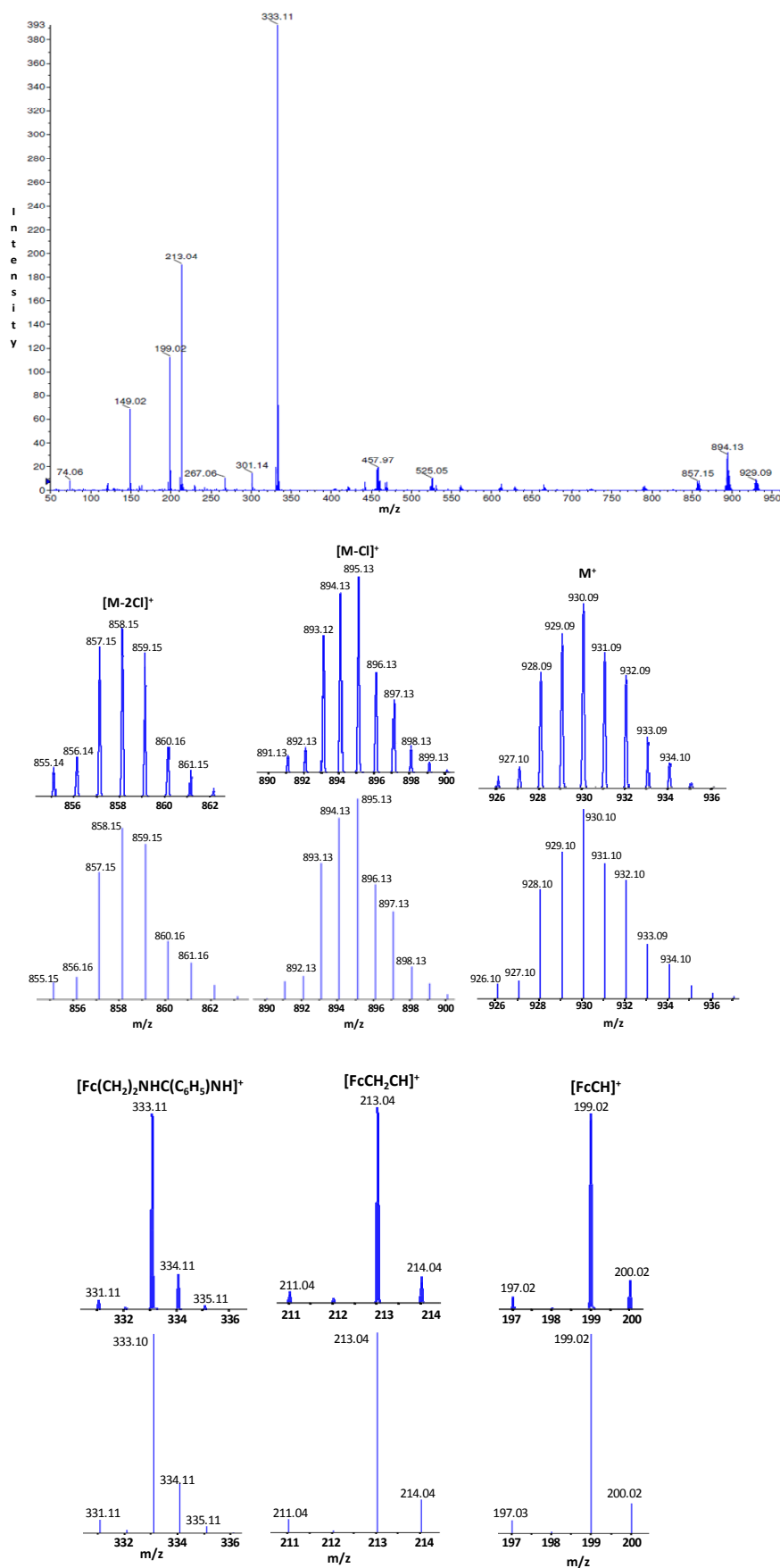


Figure S9. Mass spectrometry characterization by ESI for compound **2**. Isotopic distribution of selected peaks of **2**, experimental (top) and calculated (bottom).

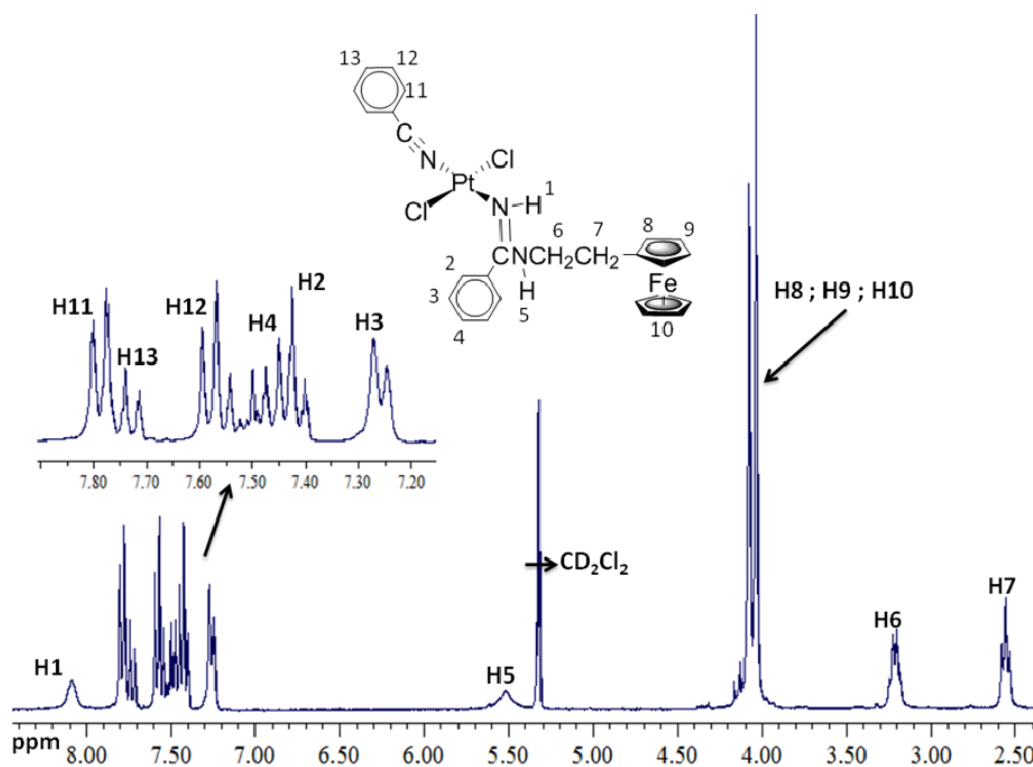


Figure S10. ^1H NMR spectrum (in CD_2Cl_2 , 300 MHz) of compound **3**.

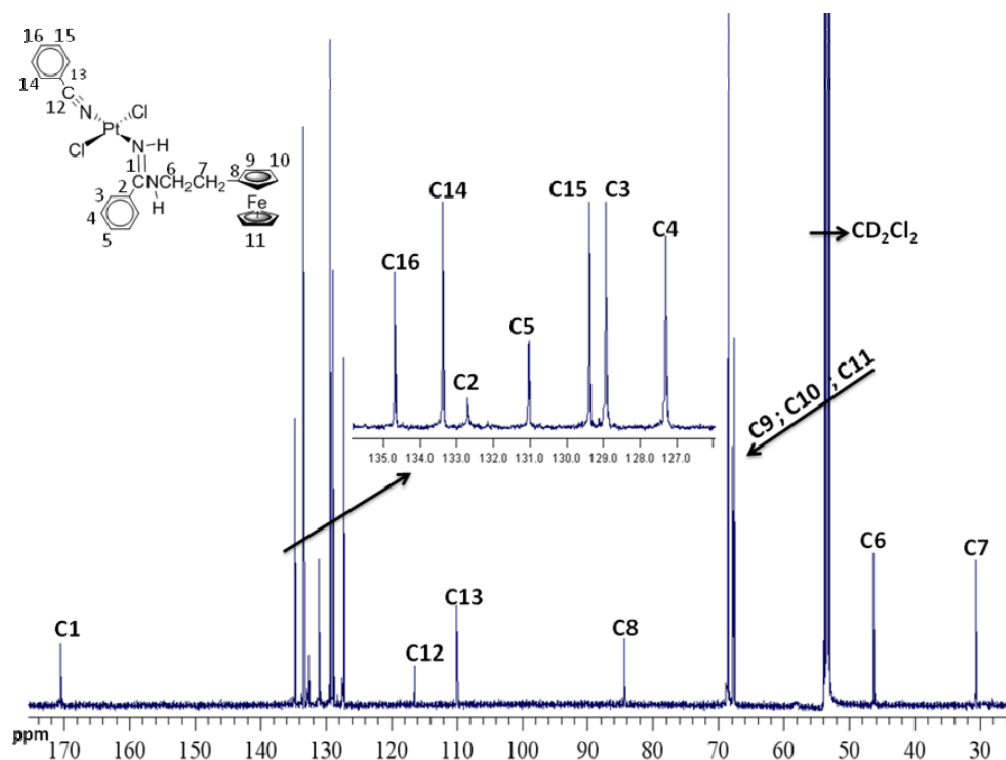


Figure S11. ^{13}C NMR spectrum (in CD_2Cl_2 , 75 MHz) of compound **3**.

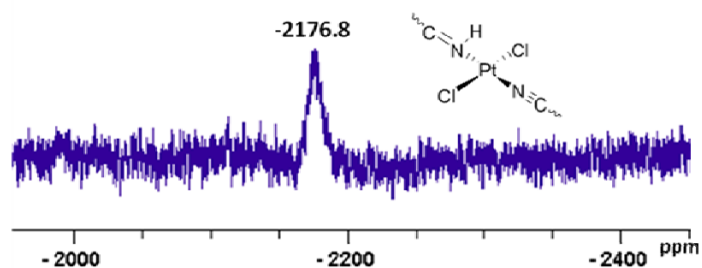


Figure S12. ^{195}Pt NMR spectrum (in CD_2Cl_2 , 64 MHz) of compound 3.

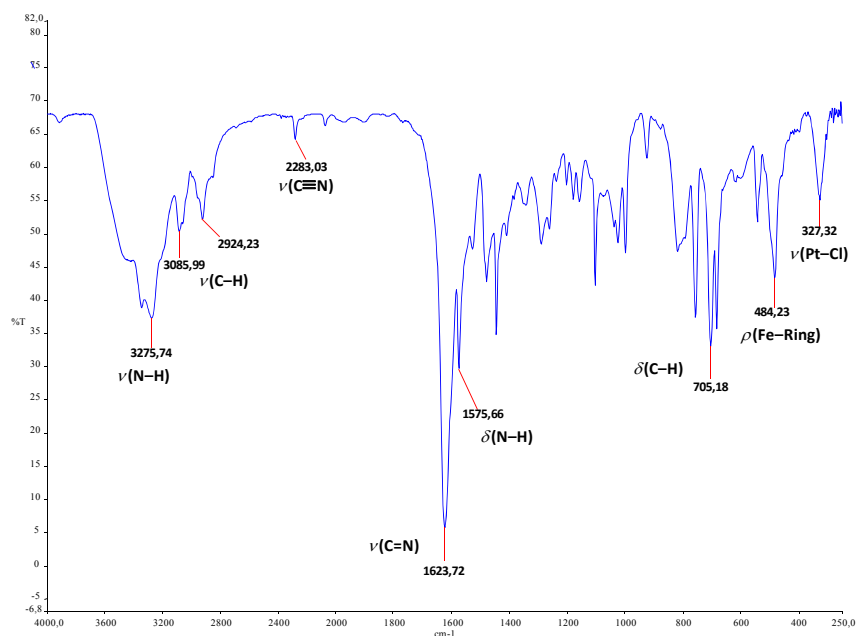


Figure S13. IR spectrum (in KBr) of compound 3.

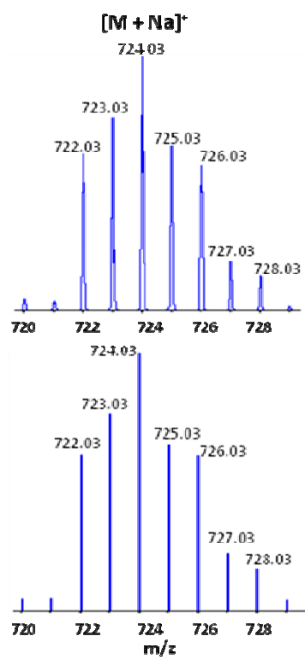


Figure S14. Mass spectrometry characterization by ESI for compound 3. Isotopic distribution: experimental (top) and calculated (bottom).

4. Crystallographic Data for Compound 2

	2
empirical formula	C ₃₈ H ₄₀ Cl ₂ Fe ₂ N ₄ Pt
FW	930.43
temp [K]	100(2)
wavelength [Å]	1.54178
cryst syst	Triclinic
space group	P-1
<i>a</i> , Å	7.8666(2)
<i>b</i> , Å	9.8807(2)
<i>c</i> , Å	12.7945(3)
α , deg	96.7530(10)
β , deg	106.7760(10)
γ , deg	111.6960(10)
<i>V</i> , Å ³	856.13(3)
<i>Z</i>	1
density (calcd), mgm ⁻³	1.805
abs coeff, mm ⁻¹	15.887
<i>F</i> (000)	460
crystal size, mm ³	0.18 x 0.14 x 0.07
θ , deg	3.73 to 69.34.
index ranges	-9 ≤ <i>h</i> ≤ 9 -11 ≤ <i>k</i> ≤ 11 - 15 ≤ <i>l</i> ≤ 14
no. of reflns collected	8987
no. of indep reflns	3057 [R(int) = 0.0314]
completeness	95.4 % (to θ = 69.34°)
absorp corr	semi-empirical from equivalents
refinement method	full-matrix least-squares on <i>F</i> ²
no. of data / restraints / params	3057 / 0 / 218
goodness-of-fit on <i>F</i> ²	1.072
final <i>R</i> indices (<i>I</i> > 2σ(<i>I</i>))	<i>R</i> ₁ = 0.0303, <i>wR</i> ₂ = 0.0751
<i>R</i> indices (all data)	<i>R</i> ₁ = 0.0311, <i>wR</i> ₂ = 0.0759
largest diff peak and hole, eÅ ⁻³	1.964 and -1.001

Table S1.- Selected crystallographic data for compound 2.

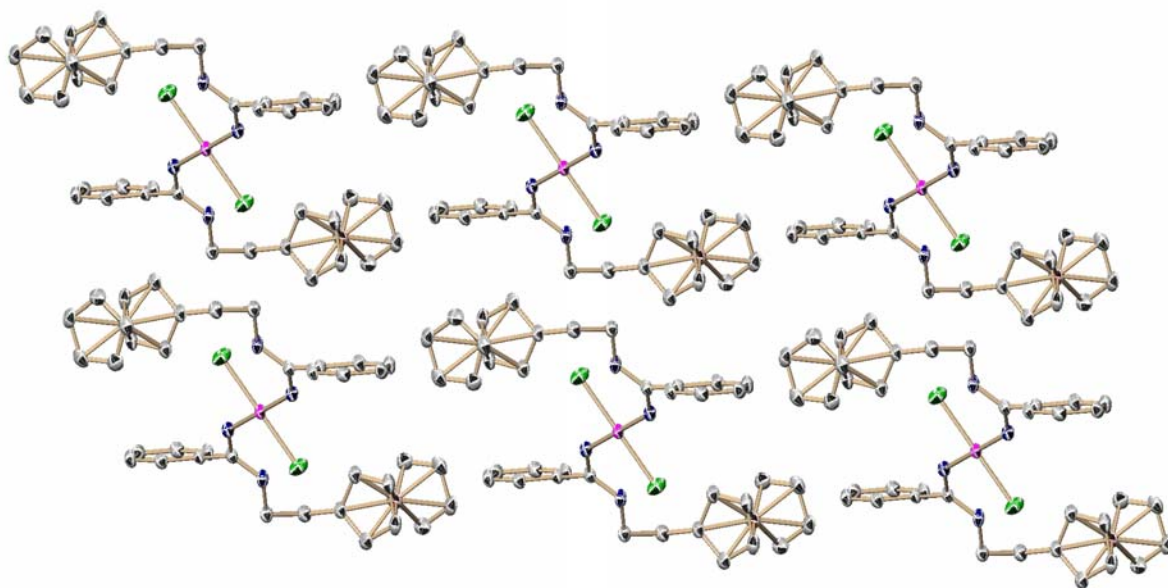


Figure S15. Crystal-packing diagram of **2** viewed along the a-axis.

5. Electrochemistry of Compound 2

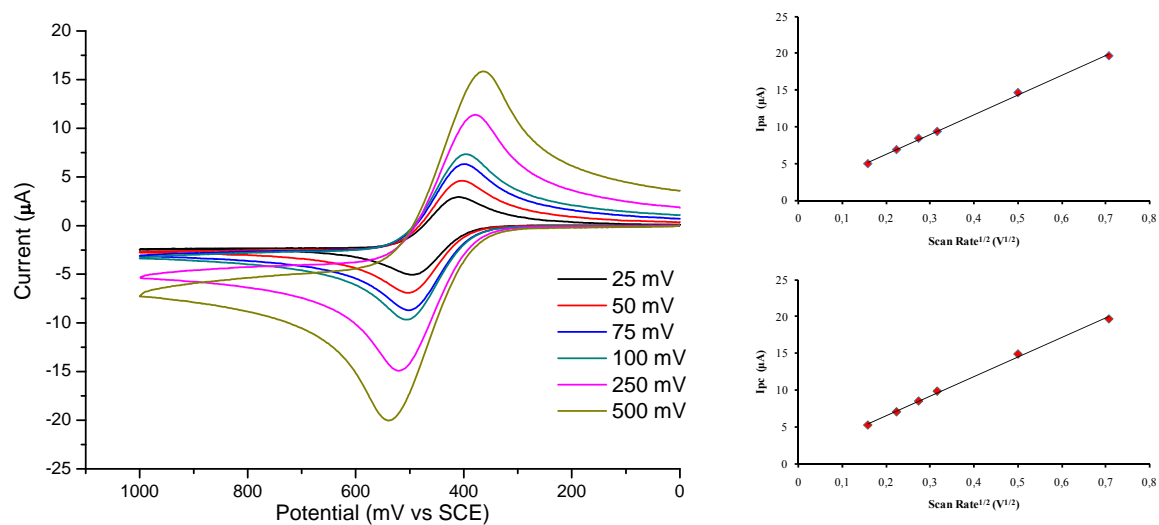


Figure S16. CV responses of compound 2 (10^{-3} M) recorded in CH_2Cl_2 containing 0.1 M TBAPF_6 , at different scan rates. Plots of I_{pa} and I_{pc} against scan rate $^{1/2}$.

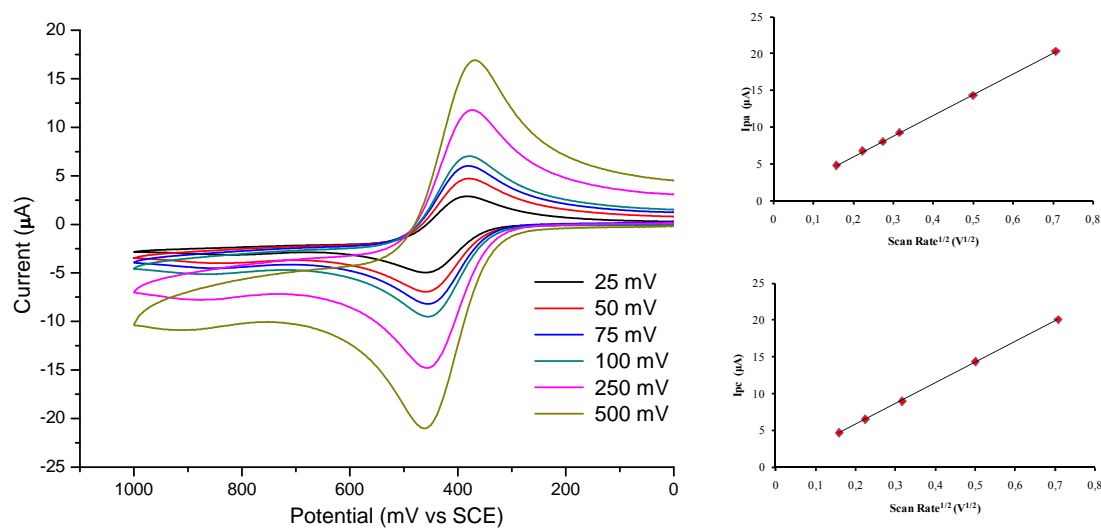
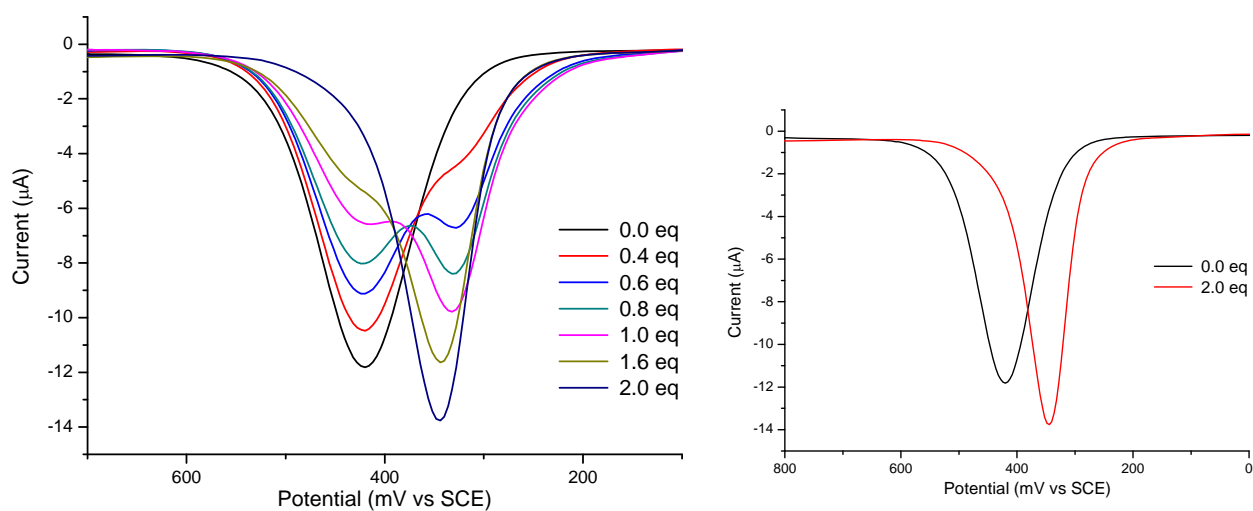
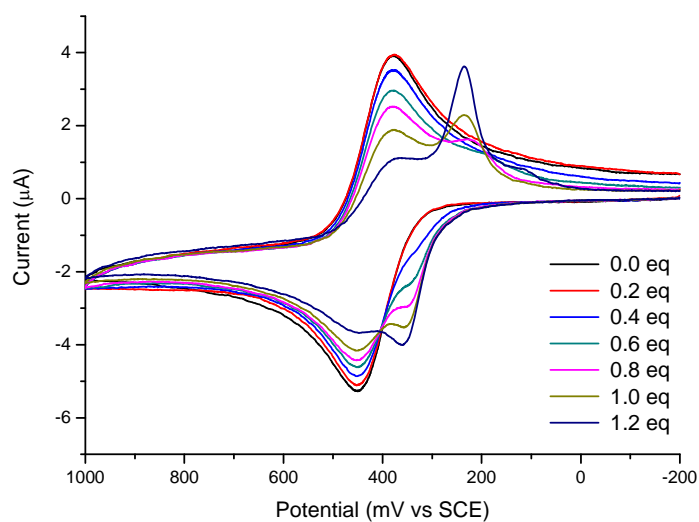


Figure S17. CV responses of compound 2 (10^{-3} M) recorded in $\text{CH}_3\text{CN}/\text{CH}_2\text{Cl}_2$ (2.5:0.5 by volume) containing 0.1 M TBAPF_6 , at different scan rates. Plots of I_{pa} and I_{pc} against scan rate $^{1/2}$.



(A)



(B)

Figure S18. Effect of H_2PO_4^- on the electrochemical responses of **2**.

SWV (A) and CV (B) responses of **2** (5×10^{-4} M) recorded in $\text{CH}_3\text{CN}/\text{CH}_2\text{Cl}_2$ (2.5:0.5 by volume) containing 0.1 M TBAPF₆, upon addition of increasing amounts of H_2PO_4^- TBA⁺. Scan rate: 100 mV s^{-1} .

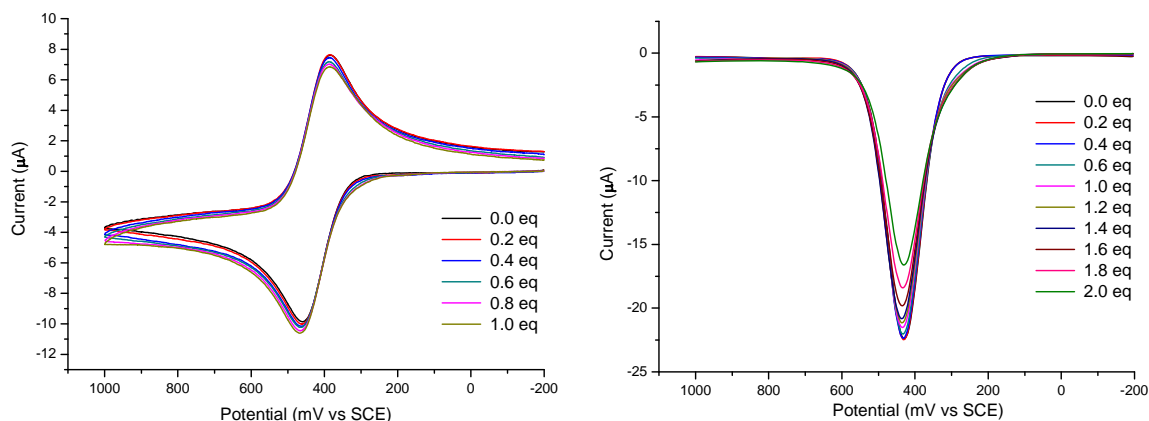


Figure S19. Effect of F^- on the electrochemical responses of **2**.

CV and SWV responses of **2** (10^{-3} M) recorded in $\text{CH}_3\text{CN}/\text{CH}_2\text{Cl}_2$ (2.5:0.5 by volume) with 0.1 M TBAPF_6 , upon addition of increasing amounts of F^- . Scan rate 100 mV s^{-1}

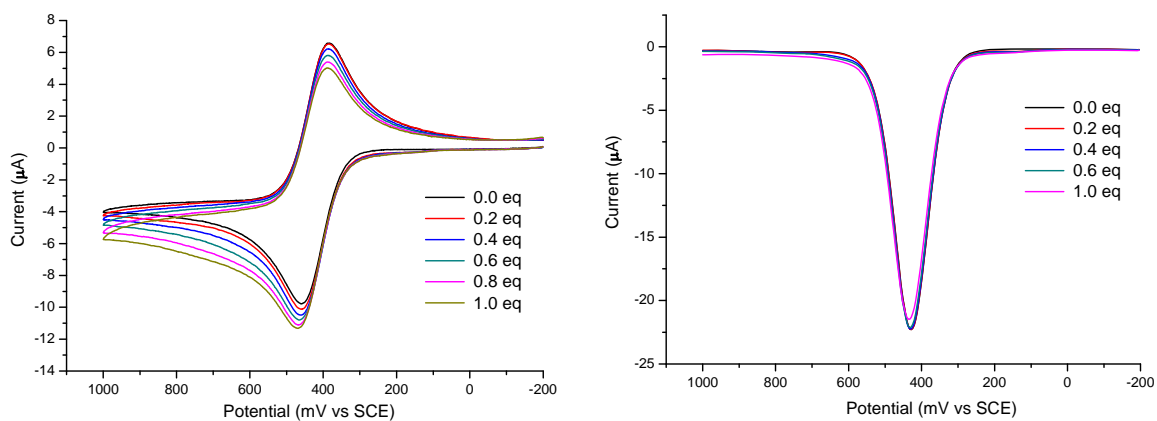


Figure S20. Effect of CH_3COO^- on the CV and SWV electrochemical responses of **2**.

SWV and CV responses of **2** (10^{-3} M) in $\text{CH}_3\text{CN}/\text{CH}_2\text{Cl}_2$ (2.5:0.5 by volume) with 0.1 M TBAPF_6 , upon addition of increasing amounts of CH_3COO^- . Scan rate: 100 mV s^{-1} .

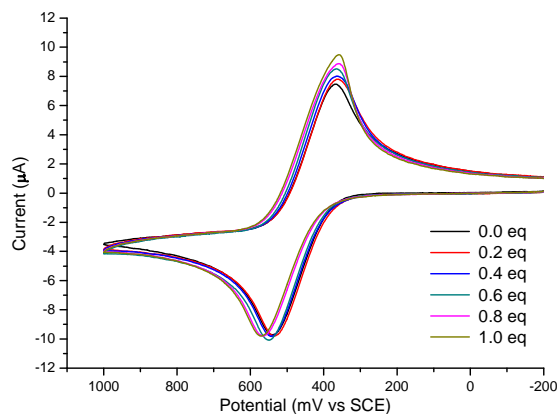


Figure S21. CV response of **2** (10^{-3} M) in CH_2Cl_2 with 0.1 M TBAPF_6 , upon addition of increasing amounts of HSO_4^- . Scan rate: 100 mV s^{-1} .

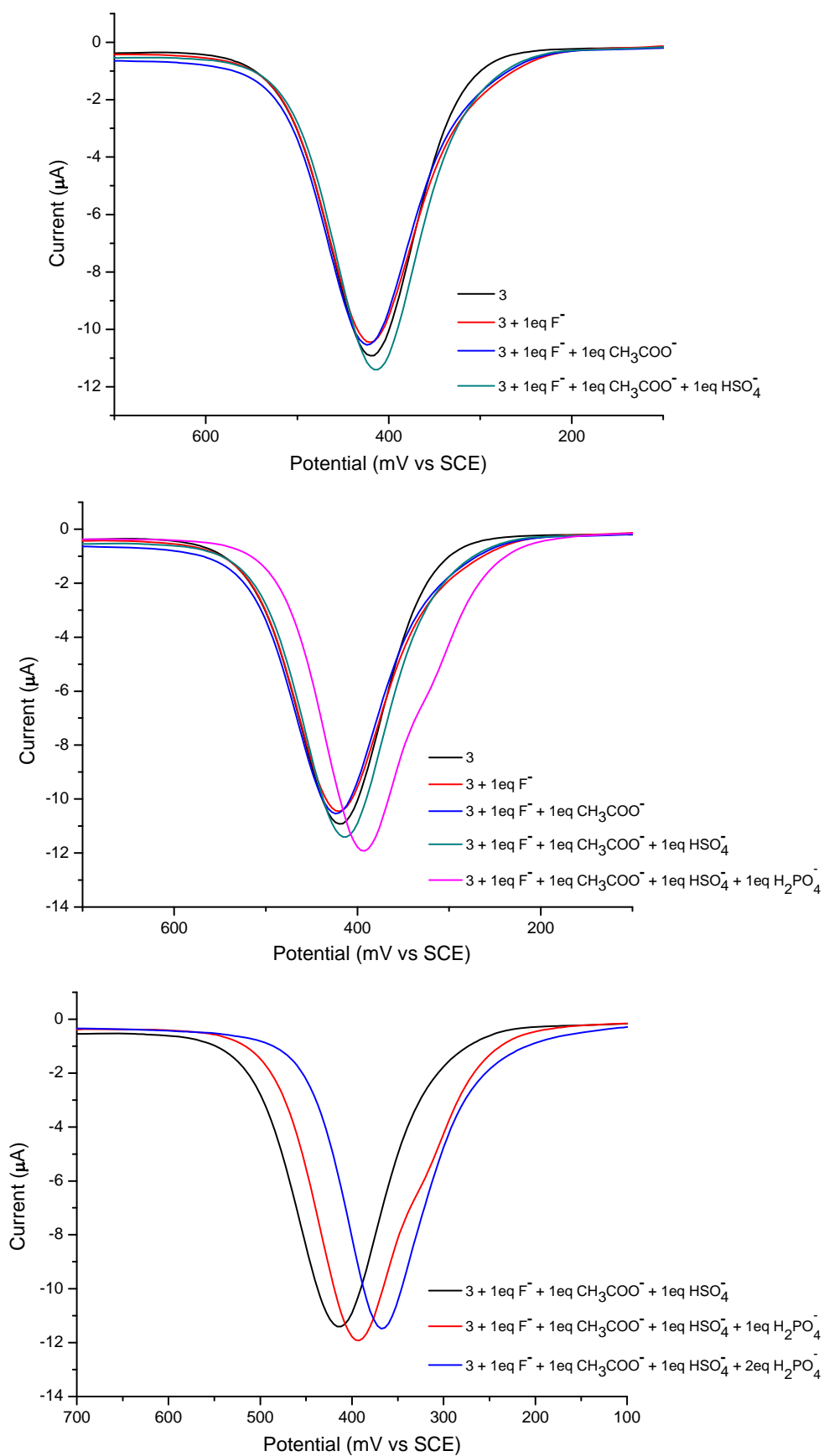


Figure S22. SWV responses of **2** in the presence of: F⁻ + CH₃COO⁻ + HSO₄⁻ + H₂PO₄⁻. Changes of the SWV response of **2** (5 × 10⁻⁴ M) in CH₃CN/CH₂Cl₂ (2.5:0.5 by volume) with 0.1 M TBAPF₆, in the absence and presence of different anions added as [n-Bu₄N]⁺ salts.

6. Electrochemistry of Compound 3

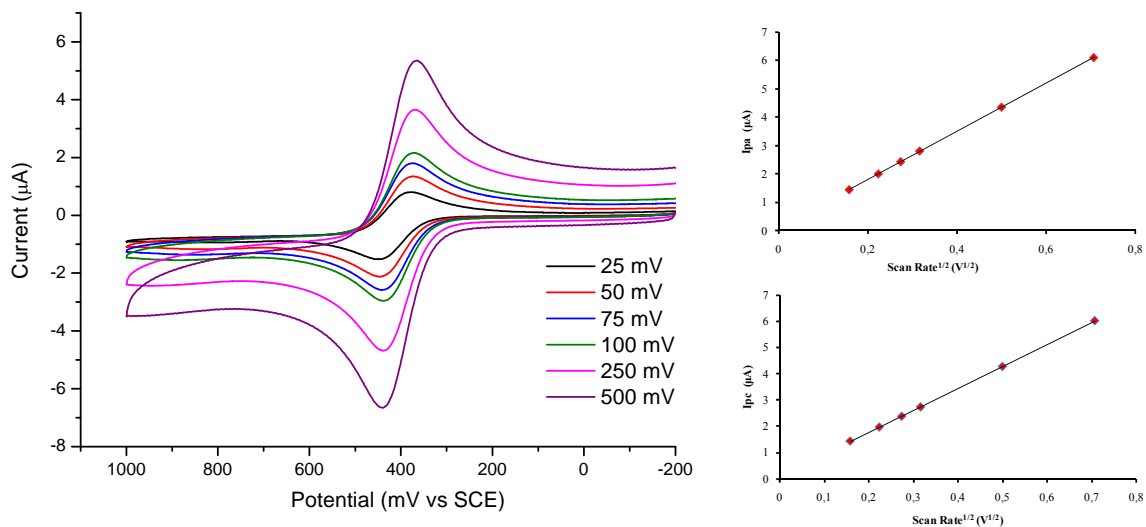


Figure S23. CV responses of compound **3** (10^{-3} M) recorded in CH_2Cl_2 containing 0.1 M TBAPF_6 , at different scan rates. Plots of I_{pa} and I_{pc} against scan rate $^{1/2}$.

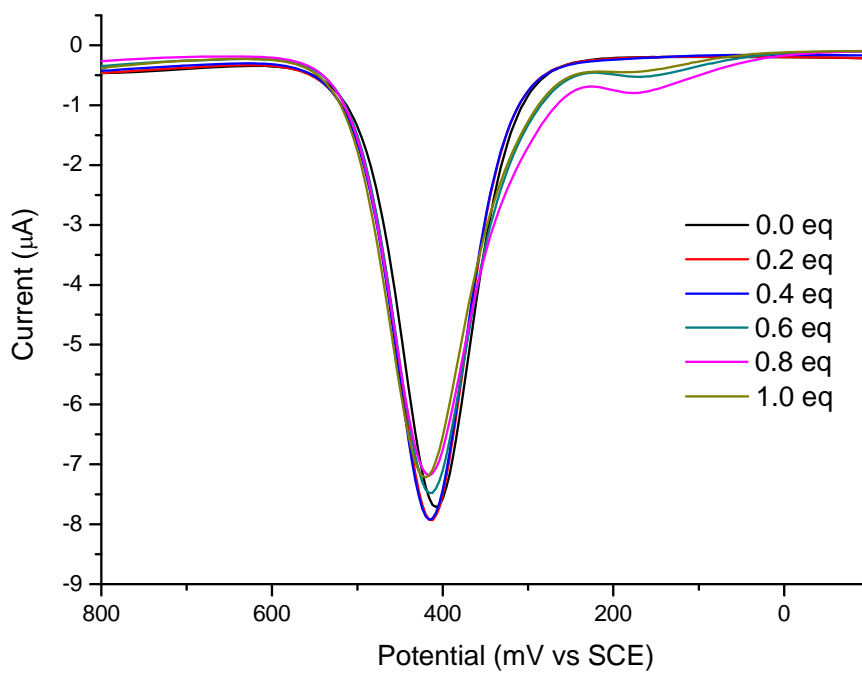


Figure S24. Effect of H_2PO_4^- on the electrochemical responses of **3**.

SWV responses of **3** (5×10^{-4} M) recorded in $\text{CH}_3\text{CN}/\text{CH}_2\text{Cl}_2$ (2.5:0.5 by volume) containing 0.1 M TBAPF_6 , upon addition of increasing amounts of H_2PO_4^- TBA $^+$.

7. References

1. Sheldrick, G. M. *SADABS* Version 2.03, Program for Empirical Absorption Correction; University of Göttingen: Germany, 1997-2001.
2. *SAINT+NT* Version 6.04; SAX Area-Detector Integration Program; Bruker Analytical X-ray Instruments: Madison, WI, 1997-2001.
3. Bruker AXS. *SHELXTL* Version 6.10, Structure Determination Package; Bruker Analytical X-ray Instruments: Madison, WI, 2000.
4. Sheldrick, G. M. *Acta Crystallogr. A*, **1990**, *46*, 467.
5. Sheldrick, G. M. *SHELXL97*, Program for Crystal Structure Refinement; University of Göttingen: Germany, 1997.
6. G. K. Anderson and M. Lin, *Inorganic Syntheses*. **1990**, *28*, 62.
7. D. Lednicer and C. R. Hauser, *Organic Syntheses*, **1973**, *5*, 578.
8. K. E. Gonsalves, R.W. Lenz, M.D. Rausch, *Appl. Organomet. Chem.*, **1987**, *1*, 81.